Theoretical analysis and computer simulation of fluorescence lifetime measurements. I. Kinetic regimes and experimental time scales

Shilong Yang and Jianshu Cao[a)]
Department of Chemistry, Massachusetts Institute of Technology, Cambridge, Massachusetts 02139

(Received 10 February 2003; accepted 6 April 2004)

The configuration-controlled regime and the diffusion-controlled regime of conformation-modulated fluorescence emission are systematically studied for Markovian and non-Markovian dynamics of the reaction coordinate. A path integral simulation is used to model fluorescence quenching processes on a semiflexible chain. First-order inhomogeneous cumulant expansion in the configuration-controlled regime defines a lower bound for the survival probability, while the Wilemski–Fixman approximation in the diffusion-controlled regime defines an upper bound. Inclusion of the experimental time window of the fluorescence measurement adds another dimension to the two kinetic regimes and provides a unified perspective for theoretical analysis and experimental investigation. We derive a rigorous generalization of the Wilemski–Fixman approximation [G. Wilemski and M. Fixman, J. Chem. Phys. **60**, 866 (1974)] and recover the $1/D$ expansion of the average lifetime derived by Weiss [G. H. Weiss, J. Chem. Phys. **80**, 2880 (1984)].
 [DOI: 10.1063/1.1756577]

I. INTRODUCTION

Reaction kinetics modulated by fluctuating environments has long been a theoretical and experimental interest.[1–16] Examples of such processes include ligand binding in proteins, slow reactions in glasses, fluorescence resonance energy transfer (FRET), and intramolecular fluorescence quenching on polymers. Recent advances in single-molecule techniques based on fluorescence spectroscopy provide powerful tools to measure the conformational structures and dynamics of synthetic and biological polymers. The FRET and intramolecular fluorescence quenching rates depend strongly on donor–acceptor or fluorophore-quencher distance, and on conformational fluctuations of polymers or biomolecules. Hence it is of great importance to study the conformation-modulated reactions, yet a unified perspective of reaction kinetics modulated by fluctuating environments have not been fully investigated. A widely used approximation scheme to calculate intrachain reactions of polymers in dilute solutions was first presented by Wilemski and Fixman,[1,2] referred here as WF approximation. Szabo, Schulten, and Schulten provided a first passage time approach to the diffusion equation with Smoluchowski boundary conditions, referred to here as the SSS theory.[3] Weiss developed a systematic perturbation analysis for diffusion-controlled reactions, which recovers the WF approximation in the lowest order.[5] Recently, Portman and Wolynes applied a variational method and proved that the WF approximation is an upper bound for the survival probability.[9]

The experimentally observed fluorescence lifetime distribution is the result of the competition between the reaction from a distribution of conformations and the diffusion between different conformational states. In the homogeneous limit, reaction is extremely slow compared to relaxation, and the system can be well approximated by equilibrium, yielding a homogeneous single-exponential decay. In the inhomogeneous limit, the survival probability is a static average over the initial configurations and has a highly nonexponential decay. Between the two limits, the relaxation process and the reaction kinetics are convoluted. The configuration-controlled regime is dominated by the reaction kinetics, and the diffusion-controlled regime is determined by the conformational relaxation process. Although complete analytic solutions are difficult, the first-order inhomogeneous cumulant expansion and the WF approximation provide exact lower and upper bounds to the real survival probability function, respectively. In the present work, we investigate these regimes for Markovian and non-Markovian fluctuations of reaction coordinates modulated by conformational fluctuations and account for the experimental time window used to monitor fluorescence. To address these two regimes and their asymptotic limits, we study a Markovian process in Sec. II and a semiflexible chain as an example of non-Markovian processes in Sec. III.

Reactions in biopolymers are often strongly coupled to internal relaxation processes, and the fluctuations of the reaction coordinate are generally non-Markovian. Reaction dynamics of biopolymers in solution can be directly probed in real time by fluorescence spectroscopy.[10–17] One important technique is intramolecular fluorescence quenching, which has been employed to measure contact formation between two residues on an unfolded polypeptide chain by Eaton's group and other groups.[18–20] By varying solvent viscosity, Eaton and his group measure the full kinetics from the inhomogeneous limit to the homogeneous limit. In Sec. III, we calculate the full kinetics of the fluorescence quenching in a semiflexible Gaussian chain with a normal mode decomposition scheme.[21] Our calculations demonstrate that the first-

[a)]Author to whom correspondence should be addressed. Electronic mail: jianshu@mit.edu

order inhomogeneous cumulant expansion and the WF approximation provide lower and upper bounds for the real survival probability, respectively.

In Sec. IV, we discuss the effects of the experimental time scale on fluorescence lifetime measurements and the unified perspective it provides. The experimental time scale here refers to the time window to monitor fluorescence. Within a very short time window, transient configurations stay close to the static configurations, independent of the relaxation rate. Such experiments can be well described within the configuration-controlled regime. For long experimental time, the configuration-controlled picture breaks down even for the slow relaxing regions. The long time kinetics is dominated by the relaxation process and is described by the diffusion-controlled regime. By varying the length of the observation time, we can observe both kinetic regimes.

In Appendix A, we generalize the WF approximation and show that the WF approximation is exact to the first order of $1/D$. In addition, we obtain the $1/D$ expansion of the average lifetime and recover the perturbation result by Weiss.[3,5] A more detailed discussion of the generalized WF approximation and its applicability criteria are addressed in paper II of this series.[22] In Appendix B, we discuss the relation between the experimental time scale and the apparent distribution of the measured quantity obtained by single-molecule experiments.

II. MARKOVIAN PROCESSES: TWO REGIMES OF LIFETIME DISTRIBUTION

Chemical reactions influenced by fluctuating environments can be described by the Smoluchowski equation coupled to a reactive sink

$$\dot{P}(t)=\mathcal{L}P(t)-KP(t). \tag{1}$$

$\mathcal{L}$ characterizes the relaxation of the fluctuating environment, and K is the first-order reaction rate coefficient. Initially, the system is prepared in thermal equilibrium, i.e., $P(0)=P_0=P_{\mathrm{eq}}$. The overall population depletion is monitored over time. Exact solutions to this equation can be obtained for only a few specific forms of the reaction rate.[3–8] Let us now discuss the calculation of the lifetime distribution function. We take the trace of the Laplace transform $\hat{P}(z)$ and write the survival probability as

$$\hat{S}(z)=\left\langle \frac{1}{z-\mathcal{L}+K}\right\rangle. \tag{2}$$

The brackets $\langle\cdots\rangle$ represent a spatial average over the equilibrium distribution. From $\hat{S}(z)$ the Laplace transform of the lifetime distribution is obtained: $\hat{f}(z)=1-z\hat{S}(z)=\langle(K-\mathcal{L})\times(z-\mathcal{L}+K)^{-1}\rangle$. The average lifetime, expressed as the first moment of the lifetime distribution function, is $\langle t\rangle=\int_0^\infty tf(t)dt=\hat{S}(0)$.

Figure 1 illustrates the configuration-controlled regime, the diffusion-controlled regime, and their corresponding limits. In the static limit, the population is depleted independently at every configuration without relaxation. In the dynamic limit, the population is depleted with a homogeneous rate while the fast relaxation maintains the population shape. Between the two limits, the kinetics can be described by the reaction dominated configuration-controlled regime and the relaxation dominated diffusion-controlled regime. Increasing the diffusion coefficient, the overall kinetics traverses from the configuration-controlled regime to the diffusion-controlled regime. Although these two regimes are not clearly separated, the boundary falls roughly into the region where the reaction and relaxation time scales become comparable.

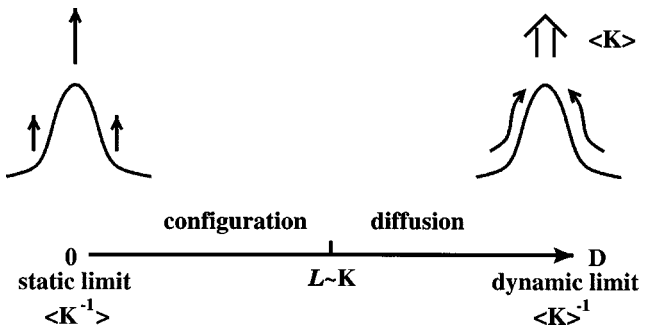

FIG. 1. An illustration of the two kinetic regimes, the configuration-controlled regime and diffusion-controlled regime, and their corresponding limits.

Let us now study the Markovian fluctuations of the reaction coordinate. The reaction rate is given in quadratic form, $K(x)=\kappa x^2+k_0$ with x the reaction coordinate. The term k_0, the nonzero decay rate at $x=0$, is necessary to remove the divergence of the static average lifetime. The fluctuation of the reaction coordinate is controlled by a one-dimensional diffusive environment, $\mathcal{L}=D\partial_x[\partial_x+\partial_x(\beta U)]$. $D=\lambda\theta$ is the diffusion coefficient, $\beta U=x^2/(2\theta)$ is the potential of mean force, and θ is the variance of the fluctuations. The relaxation is an Ornstein–Uhlenbeck process with the survival probability given by[5,7,8,23]

$$S(t)=\sqrt{\frac{4s}{(s+1)^2-(s-1)^2\exp[-2\lambda st]}}\times\exp\left\{-\left[\frac{\lambda}{2}(s-1)+k_0\right]t\right\}. \tag{3}$$

$s=\sqrt{1+4\kappa\theta/\lambda}$ represents the coupling of the time scales associated with environmental relaxation and reaction kinetics. Next we expand the square root in Eq. (3) and express the survival probability as a combination of eigenmodes. The average lifetime, i.e., the averaged sum of the eigenmode lifetimes, is

$$\langle t\rangle=\int_0^\infty S(t)dt=\sqrt{\frac{4s}{(s+1)^2}}\sum_{n=0}^{\infty}\frac{(2n-1)!!}{2^n n!}\left(\frac{s-1}{s+1}\right)^{2n}\times\frac{1}{\lambda(s-1)/2+k_0+2n\lambda s}. \tag{4}$$

The lowest eigenvalue $n=0$ yields the long-time exponent. We discuss now the different dynamic scenarios:

A. Static limit: Inhomogeneous average

The static limit case is displayed in Fig. 1. Sluggish environments such as glasses, $\mathcal{L} \ll K$, have slow relaxation rates that depend only on the initial configuration. The survival probability is the inhomogeneous average of the survival probabilities associated with each transient configuration, $S(t)=\langle \exp[-Kt] \rangle$. In this limit, the lifetime distribution function is $f(t)=\langle Ke^{-Kt} \rangle$, and the calculation of the average lifetime requires the inhomogeneous average of the time scale for each initial configuration, $\langle t \rangle = \langle K^{-1} \rangle$. Larger experimental time windows probe the configurations that relax gradually and essentially sample the configuration-controlled regime. The effects of the experimental time window in the dynamic regimes experienced by the chain conformation are elaborated in Sec. IV.

The static limit of the survival probability with a quadratic rate is obtained in the limit of $\lambda \to 0$ in Eqs. (3)

$$S(t)=\frac{1}{\sqrt{1+2\kappa\theta t}} \exp[-k_0 t]. \tag{5}$$

The averaged lifetime is

$$\langle t \rangle = \sqrt{\frac{\pi}{2k_0\kappa\theta}} \left[1-\mathrm{Erf}\left(\sqrt{\frac{k_0}{2\kappa\theta}} \right) \right] \exp\left[\frac{k_0}{2\kappa\theta} \right]. \tag{6}$$

For $k_0 \to 0$, the survival probability has a power-law decay $S(t)=1/\sqrt{1+2\kappa\theta t}$ and a divergent average lifetime.

B. Configuration-controlled regime: Inhomogeneous cumulant expansion

The configuration-controlled regime displayed in Fig. 1 is now addressed. Environmental fluctuations in viscous solvents are greatly reduced, but not negligible. The effects of the survival probability are evaluated with an inhomogeneous first-order cumulant expansion[24]

$$\begin{aligned} S(t) &= \langle \langle e^{-\int_0^t K(\tau) d\tau} \rangle_{\mathrm{inhom}} \rangle \\ &\approx \left\langle \exp\left[-\int_0^t \langle K(\tau) \rangle_{\mathrm{inhom}} d\tau \right] \right\rangle. \end{aligned} \tag{7}$$

$\langle \cdots \rangle_{\mathrm{inhom}}$ stands for the inhomogeneous average over trajectories at a given initial configuration.

In the short time limit, expansion of the configuration-controlled rate $\langle K(\tau) \rangle_{\mathrm{inhom}}$ yields $S(t) \approx \langle \exp[-K(x_0)t - D\partial_x^2 K(x_0) t^2] \rangle$ and corresponds to a summation over the inhomogeneous Gaussian line shapes in spectroscopy.[25] The average lifetime, a weighted average over the inhomogeneous reaction times, is $\langle t \rangle \approx \langle [K(x_0)]^{-1} \times \exp[-D\partial_x^2 K(x_0)/K(x_0)^2] \rangle$.[21]

The survival probability with a quadratic reaction rate is evaluated by a first-order cumulant expansion

$$S(t)=\frac{1}{\sqrt{1+2\kappa\theta t e^{-2\lambda t}}} \exp\{-[k_0+\kappa\theta(1-e^{-2\lambda t})]t\}. \tag{8}$$

The average lifetime $\langle t \rangle = \hat{S}(0)$, is displayed in Fig. 2. The plot shows that the first-order inhomogeneous cumulant expansion is the lower bound for the exact calculation and reduces to the static limit in the limit of $D=\lambda\theta \to 0$.

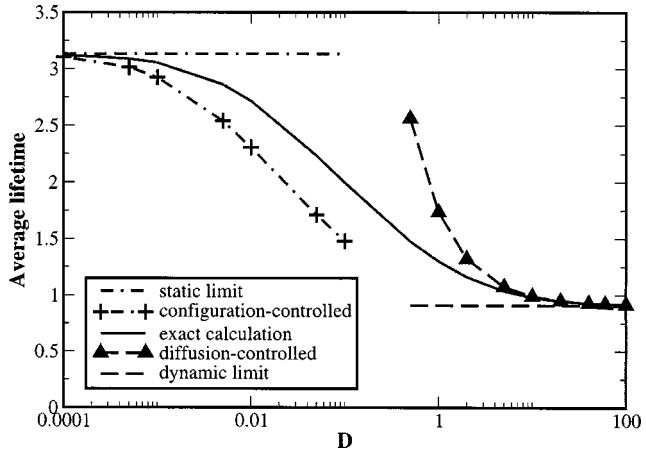

FIG. 2. The average lifetime for the Markovian fluctuations of reaction coordinate studied in Sec. II, where $\kappa=1$, $k_0=0.1$, and $\theta=1$. The diffusion coefficient D is equal to λ. The inhomogeneous cumulant expansion in configuration-controlled regime defines a lower bound for the survival probability and agrees well with the exact calculation as the reaction approaches the static limit. The WF approximation in the diffusion-controlled regime defines an upper bound and agrees with the exact calculation and the reaction approaches the dynamic limit.

C. Diffusion-controlled reaction regime: Wilemski–Fixman approximation

Let us now discuss the diffusion-controlled regime. Here, the relaxation time is shorter than the typical the reaction time. Expansion of $(z-\mathcal{L}+K)^{-1}$ followed by the ensemble average renders the survival probability

$$\begin{aligned} \hat{S}(z) &= \frac{1}{z} - \frac{1}{z^2}\langle K \rangle + \frac{1}{z^2}\langle K\hat{G}(z)K \rangle \\ &\quad - \frac{1}{z^2}\langle KG(z)K\hat{G}(z)K \rangle + \cdots. \end{aligned} \tag{9}$$

$\langle \cdots \rangle$ represents the ensemble average and $\hat{G}(z)=1/(z-\mathcal{L})$ is the Laplace transform of the Green's function $G(t)$ for the environmental relaxation. We now derive a closure for $\hat{S}(z)$. First let us separate out the asymptotic limit of $\hat{G}(z)$ as $\hat{G}(z)=\hat{G}'(z)+P_{\mathrm{eq}}/z$ with $P_{\mathrm{eq}}/z=\lim_{z\to 0}\hat{G}(z)$. The survival probability is approximated as

$$\begin{aligned} \hat{S}(z) &= \frac{1}{z} - \frac{1}{z^2}\langle K \rangle + \frac{1}{z^2}\left(\frac{\langle K \rangle^2}{z} + \langle K\hat{G}'K \rangle \right) \\ &\quad - \frac{1}{z^2}\left(\frac{\langle K \rangle^3}{z^2} + 2\langle K\hat{G}'K \rangle \frac{\langle K \rangle}{z} + \langle K\hat{G}'K\hat{G}'K \rangle \right) + \cdots \\ &\approx \frac{1}{z} - \frac{k}{z^2} + \frac{k}{z^2}\left(\frac{k}{z} + k\hat{\chi} \right) - \frac{k}{z^2}\left(\frac{k}{z} + k\hat{\chi} \right)^2 + \cdots \\ &= \frac{1+k\hat{\chi}(z)}{z[1+k\hat{\chi}(z)]+k}. \end{aligned} \tag{10}$$

$k=\langle K\rangle$ is the homogeneous average of the reaction rate and $\chi(t)=\langle KG'(t)K\rangle/k^2=\langle KG(t)K\rangle/k^2-1$. $\chi(t)$, the memory function measures the relaxational effect of the reactive system. The Laplace transform of the lifetime distribution function is obtained from Eq. (10)

$$\hat{f}(z)=\frac{k}{z(1+\hat{\chi}(z)k)+k} \tag{11}$$

with the average lifetime

$$\langle t\rangle=\hat{S}(z=0)=\frac{1+\hat{\chi}(0)k}{k}. \tag{12}$$

These results have been derived by Wilemski and Fixman using a different approach.[1,2] Let us now make several observations.

(1) $\langle KG'KG'K\rangle\approx k^3\hat{\chi}^2(z)$ applies at small reaction rates and fast relaxation times, i.e., $\hat{\chi}(0)k\ll 1$. This is consistent with the stochastic rate model discussed in Ref. 23. The survival probability was derived there from a second cumulant expansion of the stochastic rate

$$\begin{aligned}S(t)&=\langle e^{-\int K(t)dt}\rangle\\&=\exp\left[-\langle K\rangle t+\frac{1}{2}\int\langle\delta K(t_1)\delta K(t_2)\rangle dt_1dt_2+\cdots\right]\\&\approx\exp[-kt+k^2\hat{\chi}(0)t].\end{aligned} \tag{13}$$

The average lifetime, $\langle t\rangle\approx k[1-k\hat{\chi}(0)]^{-1}\approx 1/k+\hat{\chi}(0)$, recovers Eq. (12).

(2) In the homogeneous limit, $\chi(z)\to 0$, $\hat{S}(z)$ from the WF theory is $\hat{S}(z)=1/(z+k)$. Hence the survival probability decays exponentially and corresponds to a homogeneous Lorentzian line shape observed in optical spectroscopy. In the inhomogeneous limit, we have shown earlier in Sec. II B that the survival probability is given by $S(t)=\langle\exp[-K(x_0)t-D\partial_x^2K(x_0)t^2]\rangle$. This dependence corresponds to an inhomogeneous Gaussian line shape.[25]

(3) Evident from Eq. (10), the key approximation to the WF expression is $\langle KG'KG'K\rangle\approx k^3\hat{\chi}^2(z)$.[1,2] For localized reactions, $K=k(\mathbf{r}_0)\delta(\mathbf{r}-\mathbf{r}_0)$, the WF approximation and Eq. (10) are exact. This situation has been studied in the context of solvent-controlled electron transfer, where the nonadiabatic electron transfer occurs at the transition state. The diffusion-controlled electron transfer rate was first studied by Zusman and recently reexamined by Cao and Jung.[26–29]

(4) For moderate values of the diffusion coefficient, the long-time decay is still dominated by the fundamental relaxation mode and has a single-exponential decay. For finite D, the depletion rate at long time is generally different from the homogeneous average rate k, and is different from the WF approximation. A detailed discussion of the long-time decay rate is given in Sec. IV.

(5) The WF approximation in the diffusion-controlled regime provides an upper bound for the survival probability (see Ref. 9 by Portman and Wolynes). Quantitatively, the WF approximation is exact to the first order in $1/D$ for both Markovian and non-Markovian processes. A mathematical proof is given in Appendix A for an arbitrary reaction rate using the generalized WF approximation. The $1/D$ expansion of the average lifetime obtained is in agreement with Weiss's work.[3,5] A more detailed discussion of the WF approximation and its validity regime are presented in paper II of this series.[22]

The WF approximation for the quadratic reaction-rate process considered in Eq. (3) yields

$$\langle t\rangle=\frac{1}{k}+\hat{\chi}(0)\approx\frac{1}{k}+\frac{1}{\lambda}\frac{\kappa^2\theta^2}{k^2}. \tag{14}$$

The homogeneous average rate is $k=\kappa\theta+k_0$. As shown in Fig. 2, the WF approximation approaches the exact average lifetime for large λ. Direct expansion of the exact average lifetime in Eq. (4) for large λ yields

$$\begin{aligned}\langle t\rangle=&\frac{1}{k}+\frac{1}{\lambda}\frac{\kappa^2\theta^2}{k^2}-\frac{1}{\lambda^2}\frac{\kappa^2\theta^2}{2k^3}(3\kappa^2\theta^2+6\kappa\theta k_0+k_0^2)\\&+O\left(\frac{1}{\lambda^3}\right).\end{aligned} \tag{15}$$

Equation (14) reduces to the WF approximation of the average lifetime up to the first order in $1/\lambda$. The negative sign in front of the $1/\lambda^2$ term supports the fact that the WF approximation always gives the upper bound to the survival probability. This is confirmed for a non-Markovian fluctuation of the reaction coordinate by a numerical calculation in Sec. III.

D. Dynamical limit: Homogeneous average

Let us now discuss the case where the relaxation time is much shorter than the reaction time. This kinetic scenario corresponds to a phenomenological Poisson process with a homogeneous reaction rate $k=\langle K\rangle$. In this limit, the average lifetime is $1/k$, and the survival probability reduces to $\exp(-kt)$. The average lifetime approaches the dynamic limit from above as D increases, and the homogeneous average is a lower bound for the system. This limit illustrated in Fig. 2 is obtained naturally from the diffusion-controlled reaction regime discussed in the previous subsection. In the limit $\lambda\to\infty$ for the Markovian process considered in Eq. (3), the survival probability reduces to $S(t)=\exp(-kt)$, yielding the homogeneous decay.

III. NONMARKOVIAN PROCESSES: INTRAMOLECULAR FLUORESCENCE QUENCHING ON A SEMIFLEXIBLE GAUSSIAN CHAIN

Formation of a specific contact between two residues on a polypeptide chain is a fundamental process in protein folding. Fluorescence quenching has recently been employed to study the intramolecular contact in polymer chains by measuring the average lifetime of fluorescence.[18–20] In the diffusion-controlled regime, the internal relaxation of the polymer chain is controlled by solvent viscosity, and it provides an effective way to decouple the relaxation process from the quenching process.

Without explicit considerations of the excluded volume effect and geometrical constraints, ideal polymers are flexible at all length scales and are described by Gaussian statistics. However, most single molecule experiments on bio-

molecules are performed at length scales where the polymer exhibits some rigidity, and semiflexibility is key to understand the measurements of single polymer dynamics. In Ref. 21, we extended the Gaussian chain model to include the chain stiffness and studied the Brownian dynamics of the semiflexible chain with a normal mode decomposition of the Langevin equation. The equilibrium properties of semiflexible chains were studied by Kratky and Porod, Harris and Hearst, Freed, Fixman and Kovac, Ha and Thirumalai, and many others.[30–35] The non-Markovian features of the internal relaxation make it hard to solve the full kinetic equation analytically. Here we decompose non-Markovian fluctuations of the reaction coordinate into a sum of Markovian processes and investigate the coupled reaction and relaxation using path integral methods.

Eaton and co-workers measured the quenching rate for tryptophan-cysteine pairs using $K(R)=q_0\exp[-\gamma(R-a_0)]$ with $\gamma=a_0^{-1}$. The term a_0 is the contact radius, q_0 is the quenching rate at contact, and R is the reaction coordinate described by the fluorophore-quencher distance. $K(R)$ falls off exponentially as a function of the reaction coordinate. For a tryptophan-cysteine pair, $q_0=4.2\,\mathrm{ns}^{-1}$ and $a_0=0.4\,\mathrm{nm}$.[19,36] For a Gaussian chain, with two amino acids, tryptophan and cysteine attached at the end points, the equilibrium distribution of the end-to-end distance is

$$P_{\mathrm{eq}}(R)=\left[\frac{2\pi\langle R^2\rangle}{3}\right]^{-3/2}4\pi R^2\exp\left[-\frac{3R^2}{2\langle R^2\rangle}\right], \tag{16}$$

with $\langle R^2\rangle$ the mean square fluorophore-quencher distance. The normal mode representation of the end-to-end distance vector is

$$\mathbf{R}=\sum_{p=1}^{N-1}c_p\mathbf{x}_p \tag{17}$$

with $c_p=-[(-1)^p-1]/2\cos(p\pi/2N)$. The normal mode representation of the internal relaxation Smoluchowski operator $\mathcal{L}$ is

$$\mathcal{L}=\sum_{p=1}^{N-1}\frac{1}{\zeta_p}\frac{\partial}{\partial\mathbf{x}_p}\left(k_BT\frac{\partial}{\partial\mathbf{x}_p}+\lambda_p\mathbf{x}_p\right). \tag{18}$$

$\mathcal{L}$ determines the Green's function and equilibrium distribution of each normal coordinate. A detailed derivation is given in Ref. 21. The equilibrium distribution and the Green's function of the normal coordinates are

$$P_{\mathrm{eq}}(\mathbf{x}_p)=\prod_{p=1}^{N-1}\left(\frac{2\pi k_BT}{\lambda_p}\right)^{-3/2}\exp\left\{-\frac{\Sigma_{p=1}^{N-1}\lambda_p\mathbf{x}_p^2}{2k_BT}\right\} \tag{19}$$

and

$$G(\mathbf{x}_p,t|\mathbf{x}_p,t')=\prod_{p=1}^{N-1}\left[\frac{2\pi k_BT}{\lambda_p}(1-e^{-2\lambda_p/\zeta_p(t-t')})\right]^{-3/2}\times\exp\left\{-\frac{\Sigma_{p=1}^{N-1}\lambda_p[\mathbf{x}_p-\mathbf{x}_p(0)e^{-\lambda_p/\zeta_p(t-t')}]^2}{2k_BT[1-e^{-2\lambda_p/\zeta_p(t-t')}]}\right\}, \tag{20}$$

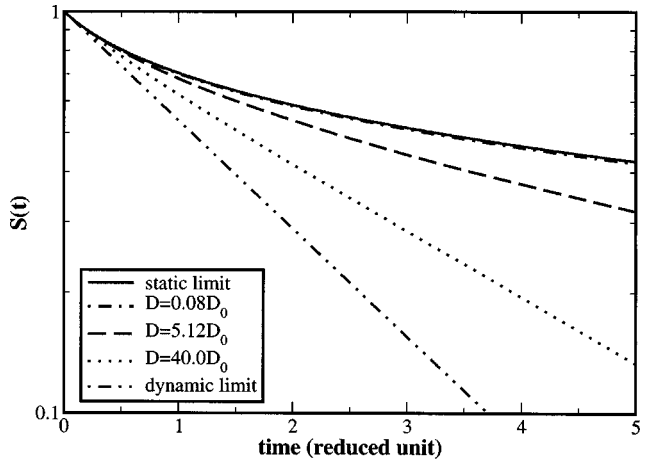

FIG. 3. Path integral simulations of the survival probability $S(t)$ for the intramolecular fluorescence quenching experiments; $a_0^2/6D_0$ is the time unit. The persistence length $L_p=2$, chain length $N=10$, and the quenching rate at contact is estimated from the experiments of Eaton *et al.* in Ref. 19 to be $q_0=5.6$. All the survival probability functions for various solvent viscosities reduce to homogeneous single-exponential decay for large observation time.

respectively. So all the normal coordinates are Markovian with different relaxation times. On the other hand, the reaction coordinate is a combination of these normal coordinates and is generally non-Markovian. In this work, we carry out path integral simulations of the fluorescence quenching process on a semiflexible chain.[27,37,38] The total time is discretized into slices $M\Delta=t$. In our simulation, initial configurations of the normal coordinates are generated according to the equilibrium distribution in Eq. (19) and propagated within each time slice according to the Green's function in Eq. (20). For each time step, we determine the end-to-end distance vector with Eq. (17) and the quenching rate accordingly. Formally, the survival probability is

$$S(t)=\lim_{M\to\infty}\int d\mathbf{X}_{M-1}\cdots\int d\mathbf{X}_0e^{-K(\mathbf{X}_{M-1})\Delta}\times G(\mathbf{X}_{M-1},(M-1)\Delta;\mathbf{X}_{M-2},(M-2)\Delta)\cdots e^{-K(\mathbf{X}_1)\Delta}G(\mathbf{X}_1,\Delta;\mathbf{X}_0,0)P_{eq}(\mathbf{X}_0) \tag{21}$$

with $\mathbf{X}$ a short notation of the normal coordinates $\{\mathbf{x}_p\}$.

In experiments, the survival probability $S(t)$ or quantum yield is monitored over a wide range of experimental time scales, and the average lifetime is obtained by integration of $S(t)$ up to the experimental time

$$\langle t\rangle=\int_0^{t_{\mathrm{exp}}}S(t)dt. \tag{22}$$

Equation (22) reduces to $\hat{S}(z=0)$ as t_{exp} approaches infinity. The configuration-controlled regime and the diffusion-controlled regime are explained in detail. We calculate survival probabilities and their corresponding average lifetimes for various solvent viscosities. The survival probability functions are shown in the master plot of Fig. 3, and the average lifetime for the full range from the static limit to the dynamic limit is plotted in Fig. 4. In both plots, a specific solvent at a viscosity of 10 cp and 293 K is taken as a reference state,

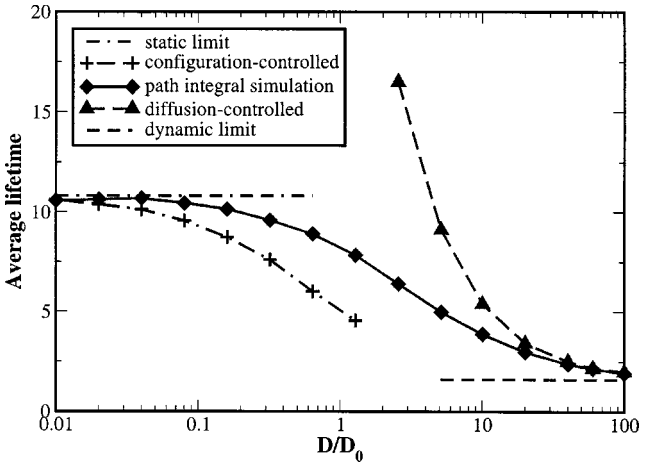

FIG. 4. The average lifetime $\langle t\rangle$ calculated by path integral simulations for a fixed experimental time $t_{\mathrm{exp}}=40$ in the reduced time unit. Other parameters are the same as in Fig. 3. The WF approximation holds for fast intrachain relaxation while the inhomogeneous cumulant expansion holds for slow intra-chain relaxation. The long-time kinetics is always described by the WF approximation for the diffusion-controlled regime.

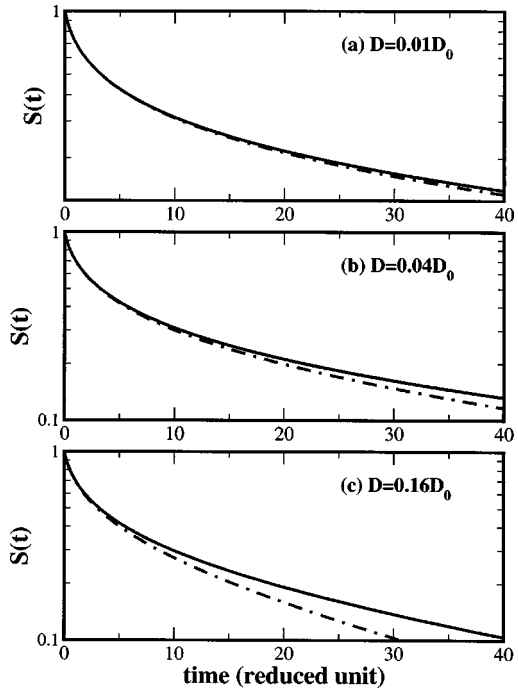

FIG. 5. Comparison of the survival probability functions calculated by path integral simulation and first-order inhomogeneous cumulant expansion. As the intra-chain relaxation becomes slow, and $t\rightarrow 0$, the inhomogeneous cumulant expansion better approximates the real survival probability. As the observation time increases, the overall kinetics is dominated by the homogeneous decay.

$a_0=0.4\,\mathrm{nm}$ is the natural length unit, and $a_0^2/6D_0\approx 25\,\mathrm{ns}$ is the corresponding time unit. In the reference state, the quenching rate at the contact is $q_0=5.6$. These numbers are used to match experimental values from Eaton's studies.[19]

The average lifetime from Eq. (22) is evaluated in a time window of $t_{\mathrm{exp}}=40$ and plotted in Fig. 4. That the average lifetime falls below the static limit is a clear indication of the reaction slowdown in the absence of sufficient relaxation. This feature is more evident in Fig. 3: The survival probability in the static limit is the upper bound for the survival probability with nonzero diffusion coefficients, and inhomogeneous effects are significant for short observation times. In the long-time limit, the kinetics is dominated by homogeneous decay.

In the configuration-controlled regime, an inhomogeneous cumulant expansion of Eq. (7) yields

$$\begin{aligned}\langle K(\tau)\rangle_{\mathrm{inhom}}=&\frac{q_0}{2}\exp\left[\left(\frac{\alpha}{2}-1\right)\gamma R_0\phi(t)+\gamma a_0\right]\\&\cdot\Bigg\{1+e^{2\gamma R_0\phi(t)}+\alpha(e^{2\gamma R_0\phi(t)}-1)\\&+|1-\alpha|\mathrm{Erf}\left(\left|\frac{(1-\alpha)\sqrt{\gamma R_0\phi(t)}}{\sqrt{2\alpha}}\right|\right)\\&-e^{2\gamma R_0\phi(t)}|1+\alpha|\\&\times\mathrm{Erf}\left(\left|\frac{(1+\alpha)\sqrt{\gamma R_0\phi(t)}}{\sqrt{2\alpha}}\right|\right)\Bigg\}\\&\text{with}\quad\alpha=\frac{\gamma\langle R^2\rangle(1-\phi^2(t))}{3R_0\phi(t)}.\end{aligned}\tag{23}$$

$\phi(t)=\langle\mathbf{R}(t)\mathbf{R}(0)\rangle/\langle\mathbf{R}^2\rangle$ is the distance–distance correlation function given in Ref. 21. Figure 5 compares inhomogeneous cumulant expansion of the survival probability and the path integral calculation. The configuration-controlled reaction provides a better approximation at lower solvent diffusion coefficients. The exact survival probability is bounded from below by inhomogeneous averaging. At larger observation time, the exact survival probability yields a homogeneous decay, consistent with our observations in Fig. 3. A more detailed discussion of the experimental time scale will be addressed in Sec. IV.

In the diffusion-controlled regime, the memory function $\chi(t)$ is obtained directly from path integral simulations and the average lifetime is evaluated with Eq. (12). Figure 4 shows that the WF approximation, $\langle t\rangle=1/k+\hat{\chi}(0)$, is an upper bound for the average lifetime. The exact result is approached from above as the relaxation rate increases. For fast diffusion, $\langle t\rangle=1/k+\hat{\chi}(0)$ converges to the dynamic limit with the order of $1/D$. The scaling of the average lifetime is demonstrated in the inset of Fig. 6. The log–log plot of $\hat{\chi}(0)$ precisely follows the $1/D$ scaling. In Fig. 6, we use the memory function $\chi(t)$ from the simulation to calculate the survival probability with the WF approximation. The numerical implementation is as follows. First, we rewrite Eq. (10) as

$$\begin{aligned}\hat{S}(z)=&\frac{1}{z+k}+k\left[\frac{1}{z+k}\hat{\chi}(z)-\hat{S}(z)\hat{\chi}(z)\right]\\&+k^2\frac{1}{z+k}\hat{\chi}(z)\hat{S}(z).\end{aligned}\tag{24}$$

Then, we invoke the inverse Laplace transform and obtain the iteration scheme

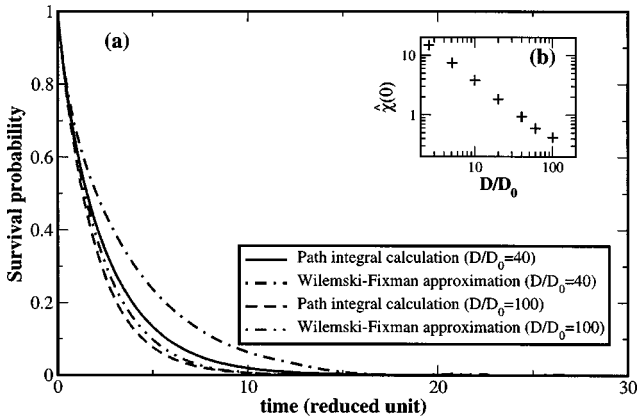

FIG. 6. (a) The survival probability functions calculated and compared for path integral simulation and WF expansion. In the long time, the WF approximation always predicts a single-exponential decay, yet with a smaller decay rate than the actual survival probability obtained from the path integral simulation. The difference in rate decreases with the diffusion coefficient. (b) A log–log plot of the contact formation time $\hat{\chi}(0)=\int_0^\infty \chi(t)dt$ vs the diffusion coefficient. $\hat{\chi}(0)$ scales as $1/D$ in the diffusion-controlled regime.

$$S(t)=e^{-kt}+k\int_0^t dt_1\int_0^{t_1} dt_2[e^{-k(t_1-t_2)}\chi(t_2) - S(t_1-t_2)\chi(t_2)]+k^2\int_0^t dt_1\int_0^{t_1} dt_2\int_0^{t_2} dt_3 \times[e^{-k(t_1-t_2)}\chi(t_2-t_3)S(t_3)]. \quad (25)$$

Figure 6 shows that the survival probability calculated using the WF approximation approaches the exact results at larger diffusion coefficients.

IV. EXPERIMENTAL TIME SCALE: A UNIFIED PERSPECTIVE

In the previous two sections, we explored the relation between the relaxation and the reaction time scales. In reality, finite experimental time windows play an important role in the kinetic interpretations. For example, in fluorescence quenching experiments we monitor the time range of population decay to obtain the average lifetime. In FRET experiments, an appropriate observation window is used to monitor the quantum yield and determine the donor–acceptor distance.[13,14]

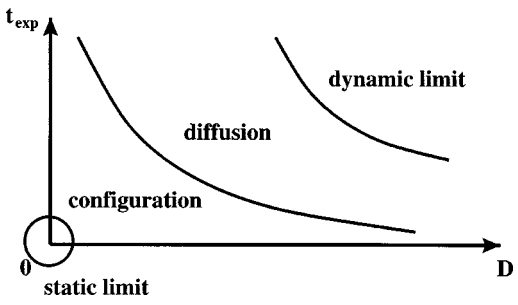

FIG. 7. An illustrative sketch of the experimental time scale effects. The boundaries drawn in the plot are only for the purpose of explanation.

The mechanism of population depletion from its dependence on D and $t_{\rm exp}$ is illustrated in Fig. 7. At small time windows, only transient configurations can be probed no matter how fast the relaxation is and the static limit is retrieved. At larger experimental times, transient configurations are no longer frozen, yet the relaxation perturbs slightly the transient configuration and the kinetics is typically in the configuration-controlled regime. The inhomogeneous cumulant expansion gives here the correction to the inhomogeneous limit. As illustrated in Fig. 7, the effective range of the configuration-controlled regime depends inversely on the relaxation rate. In the slow relaxation region, static configurations dominate the kinetics for a wide range of time. In the fast relaxation region, the static configurations relax quickly into other configurations. This behavior is clearly demonstrated in our numerical calculation for fluorescence quenching processes. The survival probabilities from the inhomogeneous cumulant expansion agree well with the exact results for small D and at short times, but the expansion fails to describe the long-time decay. That is seen clearly in Fig. 5.

Now we expand Eq. (7) to the second inhomogeneous cumulant

$$S(t)\approx\left\langle \exp\left[-\int_0^t \langle K(\tau)\rangle_{\rm inhom}d\tau+\int_0^t (t-\tau) \times\langle \delta K(\tau)\,\delta K(0)\rangle_{\rm inhom}d\tau\right]\right\rangle. \quad (26)$$

For the expansion to be valid, the second cumulant has to be smaller than the first cumulant for every initial position. Such criteria cannot be satisfied in the long-time limit. Generally speaking, in the $K\to 0$ limit, the slow-reacting population is first diffused to the fast-reacting region and then depleted at longer times. Hence the long-time decay is always dominated by the diffusion process. At small fluctuations, we evaluate the survival probability using a full cumulant expansion instead of the inhomogeneous cumulant expansion. This scenario is similar to the Gaussian stochastic rate model discussed in Ref. 23. The average lifetime is obtained from the second cumulant expansion, $\langle t\rangle=k[1-k\hat{\chi}(0)]^{-1}\approx 1/k+\hat{\chi}(0)$, which reduces to the WF results for diffusion-controlled reactions. The second cumulant expansion over the equilibrium distribution in Eq. (26) generates the same result. The transition from the short-time to the long-time behavior was discussed by Pechukas and Ankerhold in the context of Agmon–Hopfield kinetics.[39] For an ergodic system, the average of lifetime over an extreme large experimental time generates the homogeneous limit. This has been demonstrated in the numerical calculation of fluorescence quenching processes. Figures 3, 5, and 6 show that the long-time kinetics is always homogeneous regardless of the magnitude of the diffusion coefficient, yielding a single-exponential decay.

In that case, the long-time decay of the population is determined by the lowest eigenvalue of the full kinetic equation in Eq. (1).[27] Let us now define $\mathcal{L}=D\partial_x[\partial_x+\partial_x(\beta U)]$ and a corresponding Hermitian operator $\mathcal{H}=e^{\beta U/2}\mathcal{L}e^{-\beta U/2}$. $\mathcal{H}$ transforms the original kinetic equation into a Schrödinger-type equation

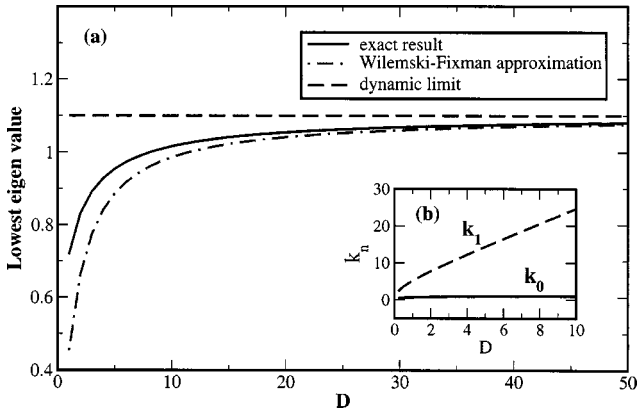

FIG. 8. (a) The asymptotic decay rate for long experimental time. The exact lowest eigenvalue and the WF approximation are calculated for the Markovian fluctuations of the reaction coordinate defined in Sec. II with the same parameters as those in Fig. 2. (b) The lowest two eigenvalues. Their gap increases almost linearly with D for large diffusion coefficients.

$$\partial_t(e^{\beta U(x)/2}P) = -K(e^{\beta U(x)/2}P) + \mathcal{H}(e^{\beta U(x)/2}P). \tag{27}$$

The lowest eigenvalue of $K-\mathcal{H}$ is k_f and the lowest eigenstate is $\psi_f(x)$. The long-time decay of the population is given by

$$\lim_{t\to 0} P(x,t) \propto \exp[-k_f t] e^{-\beta U(x)/2}\psi_f(x). \tag{28}$$

The overall population is proportional to $e^{-\beta U(x)/2}\psi_f(x)$ and decays in the long-time limit with a homogeneous rate. The dominance of the lowest eigenvalue requires a large gap between the lowest two eigenvalues $t\Delta k \gg 1$. This indicates a lower bound on the experimental time. For the Markovian case of the reaction coordinate defined in Sec. II, the eigenvalues are determined exactly as $k_n = \lambda(s-1)/2 + k_0 + 2n\lambda s$. The gap between the lowest two eigenvalues is $2\lambda s$ and is a convolution of the reaction time scale and the diffusion time scale. In the long time when $2\lambda s t \gg 1$, the population depletion is dominated by the lowest eigenvalue $k_f = \lambda(s-1)/2 + k_0$. As shown in Fig. 8, the dominant eigenvalue from the WF approximation approaches k_f from below as D increases. Both decay rates converge to $k = \langle K \rangle$ in the fast diffusion limit. The lowest two eigenvalues are plotted in the inset of Fig. 8, where the gap $k_1 - k_0 = 2\lambda s$ grows almost linearly with the diffusion coefficient at large D's.

V. CONCLUDING REMARKS

Reaction kinetics modulated by environmental fluctuations are bounded by two different regimes. In the configuration-controlled regime, the reaction process dominates, and the average lifetime becomes a weighted average over the inhomogeneous reaction time. The asymptotic limit of this regime is the static limit where the average lifetime $\langle t \rangle = \langle K^{-1} \rangle$ is an inhomogeneous average over the equilibrium distribution. In the diffusion-controlled regime, the diffusion process dominates, and in the WF approximation, $\langle t \rangle = 1/k + \hat{\chi}(0)$ is the sum of the reaction time and the diffusion time. In the dynamic limit for fast diffusion, $\langle t \rangle = 1/\langle K \rangle$ becomes the reciprocal of the homogeneous rate. The exact survival probability is bounded from below by the first-order inhomogeneous cumulant expansion and from above by the WF approximation. For comparable reaction and relaxation times, in the long-time limit the convolution of reaction kinetics and the internal relaxation process eventually reaches a fixed distribution shape and the overall reaction is characterized by a single exponential.

Variation of the experimental time of the fluorescence measurements allows people to explore various kinetic regimes from the inhomogeneous limit across the homogeneous limit. At small time windows, only static configurations are probed. At larger time windows, the relaxation process modifies the transient configurations to a configuration-controlled regime. Further increase in the measurement time probes the diffusion-controlled regime where long-time kinetics is dominated by relaxation. For ergodic systems, the long-time average yields the homogeneous limit.

In Appendix A, we generalize the WF approach to address the average lifetime. A perturbation expansion over $1/D$ of our equations reduces to the WF approximation to the first order of $1/D$. In addition, we recover the $1/D$ expansion of the average lifetime derived by Weiss.[5] In Appendix B, we discuss the relation between the experimental time scale and the apparent distribution of the measured quantities such as lifetime distribution obtained in single-molecule experiments.

Fluorescence quenching and fluorescence resonance energy transfer (FRET), can probe the details of the motions of synthetic and biological polymers. Semiflexibility, hydrodynamic interactions, excluded volume effects, and experimental time scales greatly affect their equilibrium and nonequilibrium properties. In paper II of this series,[22] we address the contour-length dependence of the average lifetime due to semiflexibility. Theoretical studies of these effects improve our understanding of the important issues related to biological functions of DNA and proteins.

ACKNOWLEDGMENTS

This research was supported by the NSF Career Award (Grant No. Che-0093210) and the Petroleum Research Fund administrated by the American Chemical Society. J.C. is a recipient of the Camille Dreyfus Teacher-Scholar Award. We would like to thank Dr. Eaton, Dr. Szabo, and Dr. Jaeyoung Sung for sending their preprints and helpful discussions.

APPENDIX A: GENERALIZED WF APPROXIMATION AND THE WEISS EXPANSION

A widely used approximation to calculate the average lifetime in the diffusion-controlled limit was first presented by Wilemski and Fixman.[1,2] As demonstrated in Secs. II and III, the WF approximation is only accurate to the first order in $1/D$, hence is useful for large diffusion coefficients. In 1980, Szabo, Schulten and Schulten presented an integral expression for the first passage time.[3] Later, Weiss obtained a $1/D$ expansion of the average lifetime based on a systematic perturbation analysis.[5] Here we generalize the WF approximation based on a perturbative expansion scheme. In paper

II of this series, we discuss the relation of this generalization with single-molecule measurements and the validity region of the WF approximation.[22]

To proceed, we consider a generic scenario described by the diffusion equation, $\partial_t P = \mathcal{L}P - KP$, where K is the reaction rate and $\mathcal{L}$ is the relaxation operator proportional to the diffusion coefficient D. We write the operator $\mathcal{L}$ as $D\mathcal{L}_0$, where $\mathcal{L}_0 = \partial_x[\partial_x + \partial_x(\beta U)]$ is the relaxation operator for unit diffusion coefficient. For simplicity, we only consider the one-dimensional case; the formalism is fully applicable to higher dimensions.

Next we employ the adjoint operator $\mathcal{L}^+$ definition which was used by Szabo, Schulten and Schulten in their solution to diffusion with Smoluchowski boundary conditions.[3] And we obtain the passage time for any given initial position x_0

$$\mathcal{L}^+ \tau(x_0) - K(x_0)\tau(x_0) = -1. \tag{A1}$$

The average lifetime is the spatial average of $\tau(x_0)$ over the equilibrium distribution

$$\langle t \rangle = \int dx_0 P_{\mathrm{eq}}(x_0)\tau(x_0). \tag{A2}$$

$P_{\mathrm{eq}} = \mathcal{N}\exp[-\beta U]$ and $\mathcal{N}$ is the normalization constant. $\mathcal{L}_0$ is not a Hermitian operator. We define a corresponding Hermitian operator: $H = \exp[\beta U/2]\mathcal{L}_0 \exp[-\beta U/2]$.[27] The adjoint operator is $\mathcal{L}^+ = \exp[\beta U/2]DH \exp[-\beta U/2]$. We define a functional space: $X = \{\phi(x) | \int \phi^2(x)dx = 1\}$ with inner product $(f,g) = \int f(x)g(x)dx$. Apparently $\phi_0(x) = \sqrt{\mathcal{N}} \times \exp[-\beta U/2] \in X$, and $H\phi_0 = 0$. The average lifetime defined in Eq. (A2) is equivalent to $\langle t \rangle = (\phi_0, (K - DH)^{-1}\phi_0)$ and the homogeneous average rate is $k = (\phi_0, K\phi_0)$. The survival probability in Laplace space is obtained as $\hat{S}(z) = (\phi_0, (z + K - DH)^{-1}\phi_0)$ in the same fashion.

We now derive the generalized WF approximation. Assuming $\{\phi_0, \phi_1, \phi_2, \ldots\}$ is an orthogonal basis of X, we can express the operators K and H as block matrices

$$K = \begin{bmatrix} K_{00} & K_{01} \\ K_{10} & K_{11} \end{bmatrix}, \quad H = \begin{bmatrix} 0 & 0 \\ 0 & H_{11} \end{bmatrix}. \tag{A3}$$

K_{00} is the homogeneous average rate k. The survival probability is

$$\begin{aligned} \hat{S}(z) &= [z + k - K_{01}(z + K_{11} - DH_{11})^{-1}K_{10}]^{-1} \\ &= \frac{1 + \hat{\Omega}(z)}{k + z[1 + \hat{\Omega}(z)]}, \end{aligned} \tag{A4}$$

where $\hat{\Omega}(z) = k^{-1}\Sigma_{n=0}^{\infty}(-1)^n D^{-(n+1)}\hat{Y}_n(z/D)$ with

$$\begin{aligned} \hat{Y}_n(z) = K_{01}[(z - H_{11})^{-1}(K_{11} - K_{10}k^{-1}K_{01})]^n \\ \times (z - H_{11})^{-1}K_{10}. \end{aligned} \tag{A5}$$

The average lifetime is

$$\langle t \rangle = \hat{S}(0) = k^{-1} + k^{-1}\hat{\Omega}(0) = \frac{1}{k} + \frac{1}{k^2}\sum_{n=0}^{\infty}\frac{(-1)^n}{D^{n+1}}\hat{Y}_n(0). \tag{A6}$$

The first moment $\hat{Y}_0(0)$ is identical to $k^2\hat{\chi}(0)$ in the WF approximation. To show this, we write the Green's function in the Laplace domain as $(z - \mathcal{L}_0)^{-1} = \exp[-\beta U/2](z - H)^{-1}\exp[\beta U/2]$. Using the block matrix representation in Eq. (A3), we evaluate $\hat{\chi}(z)$ as

$$\begin{aligned} \hat{\chi}(z) &= \frac{1}{k^2}\left\langle K\frac{1}{z - \mathcal{L}}K\right\rangle - \frac{1}{z} \\ &= \frac{1}{k^2}\left(\phi_0, K\frac{1}{z - DH}K\phi_0\right) - \frac{1}{z} \\ &= \frac{1}{Dk^2}K_{01}\frac{1}{z/D - H_{11}}K_{10}. \end{aligned} \tag{A7}$$

$\hat{\chi}(z) = (Dk^2)^{-1}\hat{Y}_0(z/D)$ reduces to $\hat{Y}_0(0)/Dk^2$ in the limit of $z \to 0$. It is ready to show that

$$\begin{aligned} (D^2k^3)^{-1}\hat{Y}_1(z/D) = k^{-3}\langle K[(z - \mathcal{L})^{-1} - z^{-1}P_{\mathrm{eq}}] \\ \times K[(z - \mathcal{L})^{-1} - z^{-1}P_{\mathrm{eq}}]K\rangle - \hat{\chi}^2(z). \end{aligned} \tag{A8}$$

A similar expansion was obtained by Weiss using a perturbative correction to the WF approximation.[5]

APPENDIX B: EXPERIMENTAL TIME SCALE AND SINGLE-MOLECULE MEASUREMENTS

In this appendix we discuss the effects of experimental time window on fluorescence lifetime measurements. We consider single-molecule quantities monitored over a fixed time window t_{exp}. A general definition of the average value within this time window is given by Gopich and Szabo as[40]

$$\overline{a} = \frac{1}{t_{\mathrm{exp}}}\int_0^{t_{\mathrm{exp}}} a[x(t)]|_{x_0}dt, \tag{B1}$$

where $x(0) = x_0$ is the initial condition. In principle, $a[x(t)]$ can be any experimentally measured quantity, for example, the FRET rate[17] or the quantum yield in FRET experiments.[14] A similar scenario is discussed for two-state dynamics of single biomolecules by Geva and Skinner.[41] Based on Hochstrasser's experiments,[17] the distribution of the measured quantity $\overline{a}$ is related to the underlying equilibrium distribution $P_{\mathrm{eq}}(x_0)$ as

$$\begin{aligned} P(\overline{a}|t_{\mathrm{exp}}) &= \int P_{\mathrm{eq}}(x_0)dx_0\left\langle \delta\left(\overline{a} - \frac{1}{t_{\mathrm{exp}}}\int_0^{t_{\mathrm{exp}}} a[x(t)]\Big|_{x_0}dt\right)\right\rangle_{\mathrm{inhom}} \\ &= \int \frac{d\omega}{2\pi}e^{i\omega\overline{a}}\left\langle\left\langle \exp\left[-\frac{i\omega}{t_{\mathrm{exp}}}\int_0^{t_{\mathrm{exp}}} a[x(t)]\Big|_{x_0}dt\right]\right\rangle_{\mathrm{inhom}}\right\rangle, \end{aligned} \tag{B2}$$

where the inner brackets $\langle\cdots\rangle_{\mathrm{inhom}}$ stand for the inhomogeneous average over trajectories with fixed initial configuration and the outer brackets $\langle\cdots\rangle$ denote the average over $P_{\mathrm{eq}}(x_0)$.

In the static limit, $t_{\mathrm{exp}} \to 0$, $P(\overline{a}|0) = [P_{\mathrm{eq}}(x_0)|\partial_{x_0}a(x_0)|^{-1}]_{x_0 = x_0^*}$ with $a(x_0^*) = \overline{a}$. For small

t_{exp}, the relaxation slightly perturbs the transient configuration, giving the configuration-controlled regime. As shown in Sec. II, we perform a first-order cumulant expansion over $a[x(t)]|_{x_0}$, yielding

$$P(\bar{a}|t_{\mathrm{exp}}) \approx \left\langle \delta\left(\bar{a} - \frac{1}{t_{\mathrm{exp}}} \int_0^{t_{\mathrm{exp}}} \langle a[x(t)]|_{x_0} \rangle_{\mathrm{inhom}} \right) \right\rangle. \quad \text{(B3)}$$

For large t_{exp}, the inhomogeneous cumulant expansion breaks down. We invoke the full cumulant expansion over $a[x(t)]|_{x_0}$ in Eq. (B2)

$$\lim_{t_{\mathrm{exp}} \to \infty} P(\bar{a}|t_{\mathrm{exp}}) = [2\pi\sigma^2(t_{\mathrm{exp}})]^{-1/2} \exp\left[- \frac{(\bar{a} - \langle a \rangle)^2}{2\sigma^2(t_{\mathrm{exp}})} \right]. \quad \text{(B4)}$$

$\langle a \rangle$ and $\sigma^2(t_{\mathrm{exp}}) = 2/t_{\mathrm{exp}}^2 \int_0^{t_{\mathrm{exp}}} (t_{\mathrm{exp}} - t) \langle \delta a[x(t)] \delta a[x(0)] \rangle dt$ are the mean and the variance of the distribution, respectively. The same expression was obtained by Gopich and Szabo from the central limit theorem.[40] For large t_{exp}, the integral in $\sigma^2(t_{\mathrm{exp}})$ reduces to $2\int_0^{\infty} \langle \delta a[x(t)] \delta a[x(0)] \rangle dt / t_{\mathrm{exp}}$, which is proportional to the ratio of the relaxational time scale and the experimental time scale. If $a = K(x)$ and $\sigma^2(t_{\mathrm{exp}}) \approx 2\langle K \rangle^2 \hat{\chi}(0)/t_{\mathrm{exp}}$, the homogeneous decay rate $\langle K \rangle$ is observed in the dynamic limit, $t_{\mathrm{exp}} \gg \hat{\chi}(0)$.

The above discussion agrees well with our picture illustrated in Fig. 7, where the overall kinetics is described by the diffusion-controlled regime for large experimental time window. Furthermore, the intermediate region between the static limit and the diffusion-controlled regime is described well by the configuration-controlled regime. Thus the inhomogeneous cumulant expansion is a natural bridge to link static limit and the dynamic limit.

The FRET rate and the quantum yield depend on the donor–acceptor distance and are affected by internal relaxation dynamics. The quantum yield can be directly measured, yet the FRET rate has to be determined indirectly from lifetime measurements. The lifetime distribution is related to the FRET rate

$$f(t) \approx \int P(\tilde{k}|t_{\mathrm{exp}}) \bar{k} e^{-\bar{k}t}. \quad \text{(B5)}$$

The term $f(t)$ in Eq. (C5) is an approximation valid for small experimental observation times. This condition limits the use of FRET rate as a measure of lifetime distribution.

[1] G. Wilemski and M. Fixman, J. Chem. Phys. **60**, 866 (1974).
[2] G. Wilemski and M. Fixman, J. Chem. Phys. **60**, 878 (1974).
[3] A. Szabo, K. Schulten, and Z. Schulten, J. Chem. Phys. **72**, 4350 (1980).
[4] N. Agmon and J. J. Hopfield, J. Chem. Phys. **78**, 6947 (1983).
[5] G. H. Weiss, J. Chem. Phys. **80**, 2880 (1984).
[6] R. Zwanzig, Acc. Chem. Res. **23**, 148 (1990).
[7] R. Zwanzig, J. Chem. Phys. **97**, 3587 (1992).
[8] J. Wang and P. G. Wolynes, Chem. Phys. Lett. **212**, 427 (1993).
[9] J. J. Portman and P. G. Wolynes, J. Phys. Chem. A **103**, 10602 (1999).
[10] T. Basche, W. E. Moerner, M. Orrit, and U. P. Wild, *Single Molecule Optical Detection, Imaging and Spectroscopy* (VCH, Wein Heim, 1997).
[11] X. S. Xie and J. K. Trautman, Annu. Rev. Phys. Chem. **49**, 441 (1998).
[12] L. Edman, U. Mets, and R. Rigler, Proc. Natl. Acad. Sci. U.S.A. **93**, 6710 (1996).
[13] S. Weiss, Science **283**, 1676 (1999).
[14] T. Ha, A. Y. Ting, J. Liang, W. B. Caldwell, A. A. Deniz, D. S. Chemla, P. G. Schultz, and S. Weiss, Proc. Natl. Acad. Sci. U.S.A. **96**, 893 (1999).
[15] A. A. Deniz, T. A. Laurence, G. S. Beligere, M. Dahan, A. B. Martin, D. S. Chemla, P. E. Dawson, P. G. Schultz, and S. Weiss, Proc. Natl. Acad. Sci. U.S.A. **97**, 5179 (2000).
[16] D. S. Talaga, W. L. Lau, H. Roder, J. Tang, Y. Jia, W. F. DeGrado, and R. M. Hochstrasser, Proc. Natl. Acad. Sci. U.S.A. **97**, 13021 (2000).
[17] M. Lee, J. Tang, and R. M. Hochstrasser, Chem. Phys. Lett. **344**, 501 (2001).
[18] L. J. Lapidus, W. A. Eaton, and J. Hofrichter, Proc. Natl. Acad. Sci. U.S.A. **97**, 7220 (2000).
[19] L. J. Lapidus, P. J. Steinbach, W. A. Eaton, A. Szabo, and J. Hofrichter, J. Phys. Chem. B **106**, 11628 (2002).
[20] O. Bieri, J. Wirz, B. Hellrung, M. Schutkowski, M. Drewello, and T. Kiefhaber, Proc. Natl. Acad. Sci. U.S.A. **96**, 9597 (1999).
[21] S. Yang, J. B. Witkoskie, and J. Cao, J. Chem. Phys. **117**, 11010 (2002).
[22] S. Yang and J. Cao, J. Chem. Phys. **121**, 572 (2004), following paper.
[23] S. Yang and J. Cao, J. Phys. Chem. B **105**, 6536 (2001).
[24] G. Diezemann, J. Chem. Phys. **116**, 1647 (2002).
[25] S. Mukamel, *Principles of Nonlinear Optical Spectroscopy* (Oxford University Press, Oxford, 1995).
[26] L. D. Zusman, Chem. Phys. **49**, 295 (1980).
[27] J. Cao, J. Phys. Chem. A **103**, 10571 (1999).
[28] J. Cao and Y. Jung, J. Chem. Phys. **112**, 4716 (2000).
[29] Y. Jung and J. Cao, J. Chem. Phys. **117**, 3822 (2002).
[30] O. Kratky and G. Porod, Recl. Trav. Chim. Pays-Bas **68**, 1106 (1949).
[31] G. Porod, J. Polym. Sci. **10**, 157 (1953).
[32] R. A. Harris and J. E. Hearst, J. Chem. Phys. **44**, 2595 (1966).
[33] K. F. Freed, J. Chem. Phys. **54**, 1453 (1971).
[34] M. Fixman and J. Kovac, J. Chem. Phys. **58**, 1564 (1973).
[35] B.-Y. Ha and D. Thirumalai, J. Chem. Phys. **106**, 4243 (1997).
[36] L. J. Lapidus, W. A. Eaton, and J. Hofrichter, Phys. Rev. Lett. **87**, 258101 (2001).
[37] H. Risken, *The Fokker-Planck Equation* (Springer, New York, 1984).
[38] R. P. Feynman and A. R. Hibbs, *Quantum Mechanics and Path Integrals* (McGraw–Hill, Co., New York, 1965).
[39] P. Pechukas and J. Ankerhold, J. Chem. Phys. **107**, 2444 (1997).
[40] I. V. Gopich and A. Szabo, preprint (2002).
[41] E. Geva and J. L. Skinner, Chem. Phys. Lett. **288**, 225 (1998).